Chapter 7 | An Introduction to Viscous Flows

7.1 Inviscid and Viscous Flows

In the preceding two chapters, our treatment of temperature, humidity, and wind distributions in the PBL was largely empirical and based on rather limited observations. A better understanding of vertical profiles of wind, temperature, and humidity and their relationships to the important exchanges of momentum, heat, and moisture through the PBL has been gained through applications of mathematical, statistical, and semiempirical theories. A brief description of some of the fundamentals of viscous flows and turbulence and the associated theory will be given in this and the following chapters.

For theoretical treatments, fluid flows are commonly divided into two broad categories, namely, inviscid and viscous flows. In an inviscid or ideal fluid the effects of viscosity are completely ignored, i.e., the fluid is assumed to have no viscosity, and the flow is considered to be nonturbulent. Inviscid flows are smooth and orderly, and the adjacent fluid layers can easily slip past each other or against solid surfaces without any friction or drag. Consequently, there is no mixing and no transfer of momentum, heat, and mass across the moving layers. Such properties can only be transported along the streamlines through advection. The inviscid flow theory obviously results in some serious dilemmas and inconsistencies when applied anywhere close to solid surfaces or density interfaces. Such dilemmas can be resolved only by recognizing the presence of boundary layers or interfacial mixing layers in which the effects of viscosity or turbulence cannot be ignored. Far away from the boundaries and density interfaces, however, the fluid viscosity can be ignored and the inviscid or ideal flow model provides a very good approximation to many real fluid flows encountered in geophysical and engineering applications. Extensive applications of this are given in books on hydrodynamics and geophysical fluid dynamics (Lamb, 1932; Pedlosky, 1979).

7.1.1 Viscosity and its effects

Fluid viscosity is a molecular property which is a measure of the internal resistance of the fluid to deformation. All real fluids, whether liquids or gases, have finite viscosities associated with them. An important manifestation of the effect of viscosity is that fluid particles adhere to a solid surface as they come in contact with the latter and consequently there is no relative motion between the fluid and the solid surface. If the surface is at rest, the fluid motion right at the surface must also vanish. This is called the no-slip boundary condition, which is also applicable at the interface of two fluids with widely different densities (e.g., air and water).

Within the fluid flow, viscosity is responsible for the frictional resistance between adjacent fluid layers. The resistance force per unit area is called the shearing stress, because it is associated with the shearing motion (variation of velocity) between the layers. A simple demonstration of this is provided by the smooth, streamlined, laminar flow between two large parallel planes, one fixed and the other moving at a slow constant speed, U_h, which are separated by a small distance h (see Figure 7.1a). At sufficiently small values of U_h and h, laminar flow can be maintained and the velocity within the fluid varies linearly from zero at the fixed plane to U_h at the moving plane, so that the velocity gradient $\partial u/\partial z = U_h/h$, everywhere in the flow. From observations in such a flow, Newton found the relationship that shearing stress is proportional to the rate of strain or velocity gradient (fluids following a linear relationship between the stress and the rate of strain are known as Newtonian fluids), that is,

$$\tau = \mu(\partial u/\partial z) \tag{7.1}$$

Where the coefficient of proportionality μ is called the dynamic viscosity of the fluid. In fluid flow problems, it is more convenient to use the kinematic viscosity $\nu \equiv \mu/\rho$, which has dimensions of $L^2 T^{-1}$.

In particular, for the gaseous fluids, such as air, a more rigorous theoretical derivation of the relationship between the shearing stress and velocity gradient can be obtained from the kinetic theory (Sutton, 1953), which clearly shows viscosity to be a molecular property which depends on the temperature and pressure in the fluid (this dependence is, however, weak and is usually ignored in most atmospheric applications).

Equation (7.1) is strictly valid only for a unidirectional flow. In most real flows, in general, spatial variations of velocity in different directions give rise to shear stresses in different directions. More general constitutive relations between the components of shearing stress and velocity gradient at any point in the fluid are (Kundu, 1990, Chapter 4)

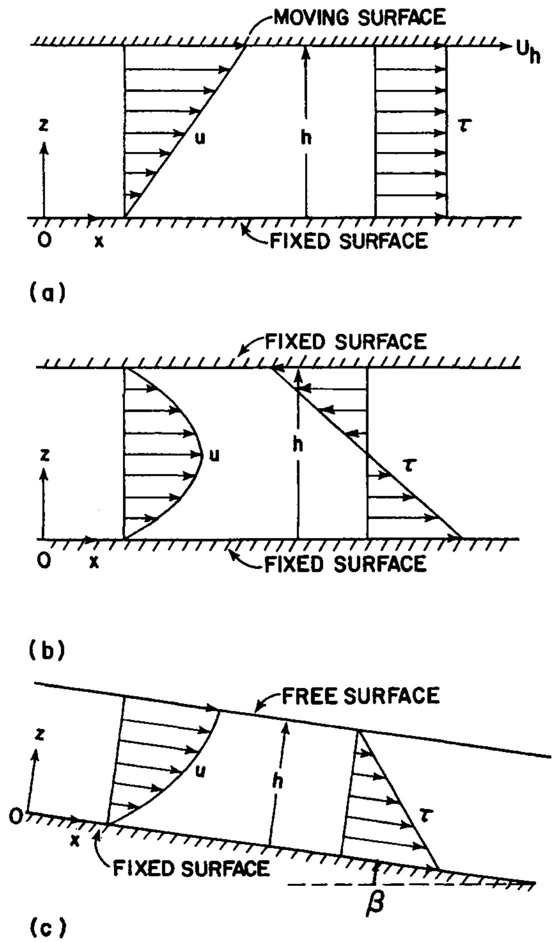

Figure 7.1 Schematics of velocity and shear stress profiles in laminar plane-parallel flows: (a) Couette flow; (b) channel flow; (c) free-surface gravity flow.

$$\begin{aligned}\tau_{xy} &= \tau_{yx} = \mu(\partial u/\partial y + \partial v/\partial x)\\ \tau_{xz} &= \tau_{zx} = \mu(\partial u/\partial z + \partial w/\partial x)\\ \tau_{yz} &= \tau_{zy} = \mu(\partial v/\partial z + \partial w/\partial y)\end{aligned} \tag{7.2}$$

in which the first member of the subscript to τ denotes the direction normal to the plane of the shearing stress and the second member denotes the direction of the stress. Equation (7.2) implies that in Newtonian fluids, shear stresses are proportional to the applied strain rates or deformations (represented by quantities in parentheses). Here, stresses and deformations are all instantaneous quantities at a point in the flow.

Another important effect of viscosity is the dissipation of kinetic energy of the fluid motion, which is constantly converted into heat. Therefore, in order to maintain the motion, the energy has to be continuously supplied externally, or converted from potential energy, which exists in the form of pressure and density gradients in the fluid.

Although the above-mentioned effects of viscosity are felt, in varying degrees, in all real fluid flows, at all times, they are found to be particularly significant only in certain regions and in certain types of flows. Such flows are called viscous flows, as opposed to the inviscid flows mentioned earlier. Examples of such flows are boundary layers, mixing layers, jets, plumes, and wakes, which are dealt with in many books on fluid mechanics (Batchelor, 1970; Townsend, 1976; Kundu, 1990).

7.2 Laminar and Turbulent Flows

All viscous flows can broadly be classified as laminar and turbulent flows, although an intermediate category of transition between the two has also been recognized. A laminar flow is characterized by smooth, orderly, and slow motion in which adjacent layers (laminae) of fluid slide past each other with very little mixing and transfer (only at the molecular scale) of properties across the layers. The main difference between the laminar flows and the inviscid flows introduced earlier is the importance of viscous and other molecular transfers of momentum, heat, and mass in the former. In laminar flows, the flow field and the associated temperature and concentration fields are regular and predictable and vary only gradually in space and time.

In sharp contrast to laminar and inviscid flows, turbulent flows are highly irregular, almost random, three-dimensional, highly rotational, dissipative, and very diffusive (mixing) motions. In these, all the flow and scalar properties exhibit highly irregular variations (fluctuations) in both time and space, with a wide range of temporal and spatial scales. For example, turbulent fluctuations of velocity in the atmospheric boundary layer typically occur over time scales ranging from 10^{-3} to 10^4 s and the corresponding spatial scales from 10^{-3} to 10^4 m – more than a millionfold range of scales. Due to their nearly random nature (there is some order, persistence, and correlation between fluctuations in time and space), turbulent motions cannot be predicted or calculated exactly as functions of time and space; one usually deals with their average statistical properties.

Although there are many examples and applications of laminar flows in industry, in the laboratory, and in biological systems, their occurrence in natural environments, particularly the atmosphere, is rare and confined to the so-called viscous sublayers over smooth surfaces (e.g., ice, mud flats, relatively undisturbed water, and tree leaves). Most fluid flows encountered in nature and engineering applications are turbulent. In particular, the various small-scale motions in the lower atmosphere are turbulent. The turbulent mixing layer may vary in depth from a few tens of meters in clear, calm, nocturnal cooling conditions to several kilometers in highly disturbed (stormy) weather conditions involving deep penetrative convection. In the upper troposphere and stratosphere also, extensive regions of clear air turbulence are found to occur. Some meteorologists consider all atmospheric motions right up to the scale of general circulation as turbulent. But, then, one has to distinguish between the small-scale three-dimensional turbulence of the type we encounter in micrometeorology, and the large-scale 'two-dimensional turbulence.' There are fundamental differences in some of their properties and mechanisms of energy transfers up or down the scales. We will only be concerned with the former here.

Turbulent, too, are the flows in upper oceans (e.g., oceanic mixed layer), lakes, rivers, and channels; practically all flows in liquid and gas pipelines; in boundary layers over moving aircraft, missiles, ships, and boats; in wakes of structures, propeller blades, turbine blades, projectiles, bullets, and rockets; in jets of exhaust gases and liquids; and in chimney and smokestack plumes. Thus turbulence is literally all around us, particularly in the form of the atmospheric boundary layer, from which we can escape only briefly. The next and the following chapters will be devoted to fundamentals of turbulence and their application to micrometeorology. But first we discuss the basic equations for viscous motion, which are valid for both laminar and turbulent flows.

7.3 Navier–Stokes Equations of Motion

Mathematical treatments of fluid flows, including those in the atmosphere, are almost always based on the equations of motion, which are mathematical expressions of the fundamental laws of the conservation of mass, momentum, and energy. For example, considerations of mass conservation in an elemental volume of fluid leads to the equation of continuity, which for an incompressible fluid, in a Cartesian coordinate system, is given by

$$\partial u/\partial x + \partial v/\partial y + \partial w/\partial z = 0 \tag{7.3}$$

The continuity equation imposes an important constraint on the fluid motion such that the divergence of velocity must be zero at all times and at every point in the flow. The assumption of incompressible fluid or flow is quite well justified in micrometeorological applications.

The application of Newton's second law of motion, or consideration of momentum conservation in an elemental volume of fluid, leads to the so-called Navier–Stokes equations, which, in a Cartesian frame of reference tied to the surface of the rotating earth with x and y axes in the horizontal and z axis in the vertical, are

$$\begin{aligned}
\frac{Du}{Dt} - fv &= -\frac{1}{\rho}\frac{\partial p}{\partial x} + \nu\nabla^2 u \\
\frac{Dv}{Dt} + fu &= -\frac{1}{\rho}\frac{\partial p}{\partial y} + \nu\nabla^2 v \\
\frac{Dw}{Dt} + g &= -\frac{1}{\rho}\frac{\partial p}{\partial z} + \nu\nabla^2 w
\end{aligned} \tag{7.4}$$

Where the total derivative and Laplacian operator are defined as

$$D/Dt \equiv \partial/\partial t + u(\partial/\partial x) + v(\partial/\partial y) + w(\partial/\partial z) \tag{7.5}$$

$$\nabla^2 \equiv \partial^2/\partial x^2 + \partial^2/\partial y^2 + \partial^2/\partial z^2 \tag{7.6}$$

The derivation of the above equations of motion is outside the scope of this text and can be found elsewhere (Haltiner and Martin, 1957; Dutton, 1976; Kundu, 1990). The physical interpretation and significance of each term can be given as follows. Terms in Equation (7.4) represent accelerations or forces per unit mass of the fluid element in the x, y, and z direction, respectively. On the left-hand sides, the first terms are called the inertia terms, because they represent the inertia forces arising due to local and advective accelerations on a fluid element. The second terms in the equations of horizontal motion represent the Coriolis accelerations or forces which apparently act on the fluid element due to the earth's rotation. The rotational term is insignificant in the equation of vertical motion and has been omitted. Instead, the gravitational acceleration term appears in the equation for vertical motion. On the right-hand sides of Equation (7.4), the first terms represent the pressure gradient forces and the second terms are viscous or friction forces on the fluid element.

When fluid viscosity or friction terms can be ignored, the equations of motion reduce to the so-called Euler's equations for an inviscid or ideal fluid. The solutions of these equations for a variety of density or temperature stratifications and initial and boundary conditions now form a rich body of literature in classical hydrodynamics (Lamb, 1932) and geophysical fluid dynamics (Pedlosky, 1979). Euler's equations of motion are considered to be adequate for describing the behavior of atmosphere and oceans outside of any boundary, interfacial, and mixing layers in which the flows are likely to be turbulent.

For a mathematical description of viscous flows, one has to use the complete set of Navier–Stokes equations, which are nonlinear partial differential equations of second order and are extremely difficult (often impossible) to solve. The combination of nonlinear inertia terms and viscous terms is responsible for the extreme difficulty and, in many cases, the intractability of solutions. Analytical solutions have been found only for limited cases of very low-speed laminar or creeping flows when nonlinear terms are absent or can be simplified. Some of these 'exact' solutions are given in the following sections in order to introduce the reader to certain classical fluid flows.

7.4 Laminar Plane-Parallel Flows

The simplest viscous flows are the steady, one-dimensional, laminar flows between two infinite parallel planes. Since velocity varies only normal to the planes and there is no motion across the planes, the inertia terms in the Navier–Stokes equations are zero. For small-scale laboratory flows, the earth's rotational effects (Coriolis terms) can also be ignored. Furthermore, choosing the x axis in the direction of flow and the z axis normal to the plane boundaries, the equations of motion reduce to

$$d^2u/dz^2 = (1/\mu)(\partial p'/\partial x) \tag{7.7}$$

which can easily be solved for different flow situations (boundary conditions). Here, p' is the modified or excess pressure obtained after subtracting the hydrostatic part from the actual pressure. For a fluid of uniform density, introduction of modified pressure eliminates the influence of gravity, so that the gravity term can be dropped from the equations of motion. The procedure of subtracting the hydrostatic part from the actual pressure is also widely used for stratified geophysical flows. For these, the pressure term in the equation of vertical motion contains the deviation of the pressure from that of the reference medium at rest which is assumed to be hydrostatic. The above procedure should not be used for liquid flows with a free surface, which are essentially forced by gravity (e.g., water flow down a sloping surface).

7.4.1 Plane-Couette flow

Consider the laminar flow between two parallel boundaries, one fixed and the other moving in the x direction at a constant velocity of U_h, separated by a small distance h, as depicted in Figure 7.1a. The relevant no-slip boundary conditions are

$$\begin{aligned} u &= 0, \quad && \text{at } z = 0 \\ u &= U_h, \quad && \text{at } z = h \end{aligned} \tag{7.8}$$

The solution of Equation (7.7) satisfying the above boundary conditions is given by

$$u = U_h \frac{z}{h} - \frac{1}{2\mu} \frac{\partial p'}{\partial x} z(h - z) \tag{7.9a}$$

or, in the dimensionless form,

$$\frac{u}{U_h} = \frac{z}{h} - \frac{h^2}{2\mu U_h} \frac{\partial p'}{\partial x} \frac{z}{h} \left(1 - \frac{z}{h}\right) \tag{7.9b}$$

Note that the velocity profile in this so-called plane-Couette flow is a combination of linear and parabolic profiles. For the special case of zero pressure gradient ($\partial p'/\partial x = 0$), the velocity profile becomes linear, i.e.,

$$u/U_h = z/h \tag{7.10}$$

and the shear stress is equal to the surface shear stress $\tau_0 = \mu U_h/h$ everywhere in the flow. This flow is entirely forced by the moving surface, or the relative motion between the two parallel surfaces, and is depicted in Figure 7.1a.

7.4.2 Plane-Poiseuille or channel flow

When both of the parallel bounding surfaces are fixed, the appropriate boundary conditions for the unidirectional flow between them are

$$\begin{aligned} u &= 0, \quad && \text{at } z = 0 \\ u &= 0, \quad && \text{at } z = h \end{aligned} \tag{7.11}$$

Then, the solution of Equation (7.7) yields a parabolic velocity profile

$$u = -\frac{1}{2\mu}\frac{\partial p'}{\partial x}z(h - z) \tag{7.12}$$

which implies a linear shear stress profile

$$\tau = \mu\frac{\partial u}{\partial z} = -\frac{1}{2}\frac{\partial p'}{\partial x}(h - 2z) \tag{7.13}$$

with the maximum value at the surface $\tau_0 = -(h/2)(\partial p'/\partial x)$. Note that in order to have a steady flow through the channel, there must be a constant negative pressure gradient in the direction of the flow. The velocity and shear stress profiles in a plane channel flow are schematically shown in Figure 7.1b.

The solution of simplified equations of motion in a cylindrical coordinate system yields similar velocity and stress profiles in a circular pipe (Hagen–Poiseuille) flow.

7.4.3 Gravity flow down an inclined plane

Here we consider a unidirectional liquid flow with a free surface or other gravity flows over uniformly sloping surfaces. The relevant equation of motion with the x axis in the direction of flow (down the slope β) and the z axis normal to the surface (Figure 7.1c) is

$$d^2u/dz^2 = -(g/\nu)\sin\beta \tag{7.14}$$

in which we have included the gravity force term but have ignored the pressure gradient. The boundary conditions are

$$\begin{aligned} u = 0, &\quad \text{at } z = 0 \\ du/dz = 0, &\quad \text{at } z = h \end{aligned} \tag{7.15}$$

The upper boundary condition implies zero shear stress at the free surface, or at $z = h$, where h represents the constant thickness of the frictional shear layer.

The solution of Equation (7.14) satisfying the above boundary conditions is given by

$$u = \frac{g\sin\beta}{2\nu}z(2h - z) \tag{7.16}$$

which is again a parabolic profile with the maximum velocity at $z = h$

$$u_h = \frac{gh^2}{2\nu} \sin \beta \tag{7.17}$$

The shear stress profile is linear with the maximum value at the surface

$$\tau_0 = \rho g h \sin \beta \tag{7.18}$$

These profiles are schematically shown in Figure 7.1c. Note that both the maximum velocity and the surface shear stress are proportional to the sine of the slope angle.

Example Problem 1

Consider fully-developed laminar flow through a circular tube of diameter d. Using the simplified forms of the equations of motion in cylindrical coordinates (r, θ, x), with the x axis coinciding with the axis of the tube and r representing the radial distance from the center of the tube, obtain expressions for the velocity and shear stress distributions across the tube and compare them with those for the plane channel flow.

Solution

Due to symmetry, all the terms in the equations of motion in r and θ directions are identically zero, because there is no motion along those directions. This implies that $\partial p/\partial r = 0$ and $\partial p/\partial \theta = 0$. The x momentum equation reduces to

$$0 = -\frac{\partial p'}{\partial x} + \frac{\mu}{r}\frac{d}{dr}\left(r\frac{du}{dr}\right)$$

or,

$$\frac{1}{r}\frac{d}{dr}\left(r\frac{du}{dr}\right) = \frac{1}{\mu}\frac{\partial p'}{\partial x}$$

Since the left-hand side of the above equation can be a function only of r, and the right-hand side can be a function only of x, it follows that both terms must be constant. Therefore, the pressure gradient along the direction of flow must be constant and pressure falls linearly along the length of the tube.

Multiplying the above equation by r and integrating with respect to r, we get

$$r\frac{du}{dr} = \frac{r^2}{2\mu}\frac{\partial p'}{\partial x} + A$$

or,

$$\frac{du}{dr} = \frac{r}{2\mu}\frac{\partial p'}{\partial x} + \frac{A}{r}$$

in which the integration constant $A = 0$, because $du/dr = 0$ at $r = 0$ (velocity is maximum at the center of the tube). Integrating the above equation again gives

$$u = \frac{r^2}{4\mu}\frac{\partial p'}{\partial x} + B$$

where B is another integration constant, which can be evaluated from the no-slip boundary condition at the tube surface ($r = d/2$, $u = 0$) as $B = -(d^2/16\mu)\partial p'/\partial x$. Thus, the velocity distribution in the tube is given by

$$u = -\frac{1}{16\mu}\frac{\partial p'}{\partial x}(d^2 - 4r^2)$$

The corresponding shear stress distribution is given by

$$\tau = \mu\frac{\partial u}{\partial r} = \frac{r}{2}\frac{\partial p'}{\partial x}$$

with the maximum value at the tube surface $\tau_0 = 0.25d\,\partial p'/\partial x$.

Note that the velocity profile across the tube cross-section is parabolic and the shear stress profile is linear, similar to those for the plane channel flow given by Equations (7.12) and (7.13). The volumetric flow rate is given by

$$Q = \int_0^{d/2} 2\pi r u dr = -\frac{\pi}{8\mu}\frac{\partial p'}{\partial x}\int_0^{d/2} r(d^2 - 4r^2)dr$$

or,

$$Q = -\frac{d^4}{128\mu}\frac{\partial p'}{\partial x}$$

The average velocity through the tube can be obtained by dividing the above volume flow rate by the cross-sectional area of the tube, i.e.,

$$V = -\frac{d^2}{32\mu}\frac{\partial p'}{\partial x}$$

7.5 Laminar Ekman Layers

In this section, we consider the laminar Ekman boundary layers on rotating surfaces, particularly those of the atmosphere and oceans, aside from the conditions of their existence.

7.5.1 Ekman layer below the sea surface

First, we examine the problem of drift currents set up at or just below the sea surface, in response to a steady wind stress forcing. For the sake of simplicity, surface waves are being ignored and so are the horizontal pressure and density gradients in water. Then, the equations of horizontal motion [Equation (7.4)] reduce to

$$-fv = \nu \frac{d^2u}{dz^2}; \quad fu = \nu \frac{d^2v}{dz^2} \tag{7.19}$$

Assuming the x axis is in the direction of the applied surface stress τ_0 and the z axis is pointed vertically upward, the boundary conditions to be satisfied are

$$\begin{aligned} &\mu\frac{du}{dz} = \tau_0, \quad \mu\frac{\partial v}{\partial z} = 0, \quad \text{at } z = 0 \\ &u \to 0, \quad v \to 0, \quad \text{as } z \to -\infty \end{aligned} \tag{7.20}$$

The two equations can be combined in a single equation for the complex current $c = u + iv$, by multiplying the second part of Equation (7.19) by $i = \sqrt{-1}$ and adding it to the first. The resulting equation

$$d^2c/dz^2 - i(f/\nu)c = 0 \tag{7.21}$$

has the solution satisfying the boundary condition at infinity

$$c = u + iv = A\exp[a(1 + i)z] \tag{7.22}$$

where $a = (f/2\nu)^{1/2}$ and A is a complex constant determined from the surface boundary condition to be

$$A = (\tau_0/2a\mu)(1 - i) \tag{7.23}$$

Substituting from Equation (7.23) into Equation (7.22) and separating into real and imaginary parts, one obtains

$$\begin{aligned} u &= (\tau_0/\sqrt{2}a\mu)e^{az}\cos(az - \pi/4) \\ v &= (\tau_0/\sqrt{2}a\mu)e^{az}\sin(az - \pi/4) \end{aligned} \tag{7.24}$$

Note that according to the above solution, the current has a maximum speed of $\tau_0/\sqrt{2}a\mu$ at the surface and is directed 45° in a clockwise sense from the direction of applied stress. With increasing depth (negative z) the current speed decreases exponentially and the current direction rotates in a clockwise sense. A common method of representing the current speed and direction as a function of depth below the surface is to plot a velocity hodograph as in Figure 7.2a. Note that the velocity hodograph represented by Equation (7.24) is a spiral; it is known as the Ekman spiral, after the Swedish oceanographer V.W. Ekman who first derived the above solution.

Although the induced current theoretically disappears only at an infinite depth, in practice, the influence of surface stress forcing becomes insignificant at a depth of the order of $a^{-1} = (2\nu/f)^{1/2}$. Conventionally, the Ekman layer depth h_E is defined as the depth where the current direction becomes exactly opposite to the surface current direction. According to Equation (7.24), this happens at $z = -\pi a^{-1}$, so that $h_E = \pi(2\nu/f)^{1/2}$; at this depth the magnitude of the current has fallen to a small fraction ($e^{-\pi} \cong 0.04$) of its surface value.

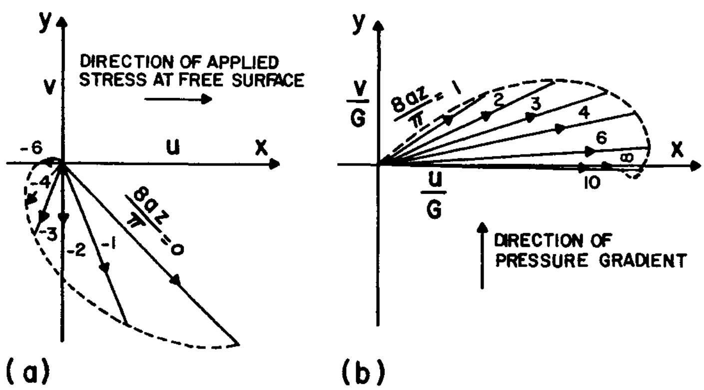

Figure 7.2 Velocity hodographs in laminar Ekman layers: (a) below free surface where tangential stress is applied; (b) above a rigid surface where a constant pressure gradient is applied. [From Batchelor (1970).]

Another parameter of interest is the net transport of water across vertical planes due to induced currents in the Ekman layer, which is given by the integral

$$\int_0^{-\infty} (u + iv)dz = -i(\tau_0/\rho f) \tag{7.25}$$

Thus, the net transport is to the right and normal to the direction of applied stress; it is proportional to the stress, but independent of fluid viscosity. In fact, the above result also follows directly from the integration of the equations of motion (7.19) after expressing the viscous terms in the form of the vertical gradients of stresses, viz., $d\tau_{zx}/dz$ and $d\tau_{zy}/dz$.

7.5.2 Ekman layer at a rigid surface

Another example of an Ekman layer is that due to a uniform pressure gradient in the atmosphere near the surface or in the ocean near the bottom boundary. For the sake of simplicity, again, the surface is assumed to be flat and uniform and the flow is considered laminar. In the absence of inertia terms, the equations of motion to be solved are

$$\begin{aligned} -fv &= -\frac{1}{\rho}\frac{\partial p}{\partial x} + \nu\frac{d^2u}{dz^2} \\ fu &= -\frac{1}{\rho}\frac{\partial p}{\partial y} + \nu\frac{d^2v}{dz^2} \end{aligned} \tag{7.26}$$

Expressing pressure gradients in terms of geostrophic velocity components using Equation (6.1), Equation (7.26) can be written as

$$\begin{aligned} -f(v - V_g) &= \nu(d^2/dz^2)(u - U_g) \\ f(u - U_g) &= \nu(d^2/dz^2)(v - V_g) \end{aligned} \tag{7.27}$$

in which U_g and V_g have been taken as height-independent parameters, ignoring any small variations of these over the small depth of the Ekman layer. The appropriate boundary conditions, assuming geostrophic balance outside the Ekman layer, are

$$\begin{aligned} &u = 0 \quad v = 0, \quad \text{at } z = 0 \\ &u \to U_g, \quad v \to V_g, \quad \text{as } z \to \infty \end{aligned} \tag{7.28}$$

The previous set of equations [Equation (7.27)] is similar to Equation (7.19), and the solution, following the earlier solution, is

$$\begin{aligned} u - U_g &= -e^{-az}[U_g \cos(az) + V_g \sin(az)] \\ v - V_g &= e^{-az}[U_g \sin(az) - V_g \cos(az)] \end{aligned} \tag{7.29}$$

This is a general solution which is independent of the orientation of the horizontal coordinate axes. A more specific and simpler solution is usually given by taking the x axis to be oriented with the geostrophic wind vector, so that $U_g = G$ and $V_g = 0$ in this geostrophic coordinate system and Equation (7.29) can be written as

$$\begin{aligned} u &= G[1 - e^{-az} \cos(az)] \\ v &= Ge^{-az} \sin(az) \end{aligned} \tag{7.30}$$

The normalized wind hodograph (Ekman spiral), according to Equation (7.30), is shown in Figure 7.2b. It shows that, in the northern hemisphere, the wind vector rotates in a clockwise sense as the height increases, and that the angle between the surface wind or stress and the geostrophic wind is 45° (this is also the cross-isobar angle of the flow near the surface), irrespective of stability. Figure 7.3a shows the profiles of the normalized velocity components u/G and v/G as functions of the normalized height az. Both the components increase approximately linearly with height above the surface, attain their maxima at different heights and then oscillate around their geostrophic values with decreasing amplitude of oscillation as height increases, reflecting the influence of the e^{-az} factor.

It should be recognized that although the spiral shape of the velocity hodograph remains invariant with the rotation of horizontal (x–y) coordinate axes, the velocity component profiles and their expressions depend on the choice of the coordinate axes. For example, Equations (7.30) are the particular expressions of velocity components in the geostrophic coordinate system. In the surface-layer coordinate system with the x axis along the near-surface wind, which is more frequently used in micrometeorology, it is found that $U_g = G/\sqrt{2}$, $V_g = -G/\sqrt{2}$, and the horizontal velocity components from Equation (7.29) are given as

$$\begin{aligned} u &= \frac{G}{\sqrt{2}} - \frac{G}{\sqrt{2}} e^{-az}[\cos(az) - \sin(az)] \\ v &= -\frac{G}{\sqrt{2}} + \frac{G}{\sqrt{2}} e^{-az}[\cos(az) + \sin(az)] \end{aligned} \tag{7.31}$$

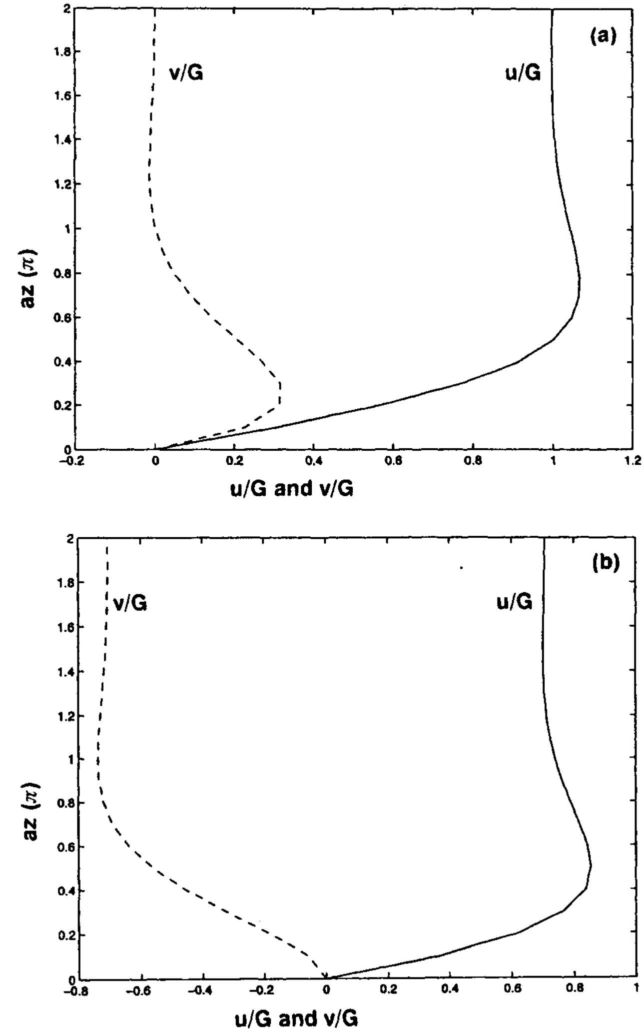

Figure 7.3 Horizontal velocity component profiles in the laminar Ekman layer in (a) the geostrophic coordinate system, and (b) the surface-layer coordinate system. Velocity components are normalized by geostrophic wind speed G, while az is the normalized height.

These component profiles (normalized by G) are represented in Figure 7.3b as functions of az and can be contrasted with those of Figure 7.3a based on the geostrophic coordinate system.

The Ekman layer depth again is given as $h_E = \pi(2\nu/f)^{1/2}$, which in middle latitudes ($f \cong 10^{-4}\ \mathrm{s}^{-1}$) is only about 1.7 m (the depth of the wind-induced oceanic Ekman spiral is about 0.5 m). There is no observational evidence for the occurrence of such shallow laminar Ekman layers in the atmosphere or oceans. Therefore, the above solutions would be of academic interest only, unless ν is replaced by a much higher effective (eddy) viscosity K to match the theoretical Ekman layer depth with that observed under a given set of conditions. Ekman (1905) originally proposed this method or procedure for estimating the 'virtual viscosity' from the observed depth, h, of frictional influence as $K = fh^2/2\pi^2$. Even then, certain features of the above solution remain inconsistent with observations. For example, the cross-isobar angle of the atmospheric flow near the surface is highly variable, as discussed in Chapter 6, and the theoretical value of $\alpha_0 = 45°$ is found more as an exception rather than the rule. Another inconsistent feature of the Ekman solution is an almost linear velocity profile near the surface, while observations indicate approximately logarithmic or log-linear velocity profiles in the surface layer. Slightly modified solutions with an appropriate choice of effective viscosity and lower boundary conditions (in the form of specified wind speed or wind direction) at the top of the surface layer have been given in the literature and largely remove the above-mentioned limitations and inconsistencies of the original Ekman solution and show better correspondence with observed wind profiles.

Example Problem 2

For the barotropic atmospheric boundary layer, the equations for the mean horizontal motion are similar to Equations (7.27) with ν replaced by an apparent or effective viscosity K. Obtain a solution to the same in a surface-layer coordinate system with the x axis oriented along the near-surface wind, using a lower boundary condition based on the observed near-surface wind U_s at $z = h_s$. Then, calculate the component velocity profiles and the boundary layer height for the following parametric values:

$$G = 10\ \mathrm{m\ s^{-1}};\quad U_s = 7\ \mathrm{m\ s^{-1}};\quad h_s = 10\ \mathrm{m};$$
$$K = 2\ \mathrm{m^2\ s^{-1}};\quad f = 10^{-4}\ \mathrm{s^{-1}}$$

Solution

The equations of mean motion for the PBL over a homogeneous surface are:

$$-\rho f(V - V_g) = \frac{d\tau_{zx}}{dz}$$
$$\rho f(U - U_g) = \frac{d\tau_{zy}}{dz}$$

Expressing $\tau_{zx} = \rho K dU/dz$ and $\tau_{zy} = \rho K dV/dz$, in analogy with their expressions (7.2) for laminar flows, and assuming K to be independent of height (a rather gross assumption), one can write the above equations in the form

$$\frac{d^2U}{dz^2} + \frac{f}{K}(V - V_g) = 0$$

$$\frac{d^2V}{dz^2} - \frac{f}{K}(U - U_g) = 0$$

For the barotropic PBL in which U_g and V_g are independent of height, the above two equations can be combined into one equation for the complex ageostrophic wind

$$\frac{d^2W_a}{dz^2} - \left(\frac{if}{K}\right)W_a = 0$$

where,

$$W_a = (U - U_g) + i(V - V_g)$$

The boundary conditions to be satisfied by the solution to the above equation are:

$$\begin{aligned} &\text{at } z = h_s,\ U = U_s, \text{ and } V = 0 \\ &\text{as } z \to \infty,\ U \to U_g \text{ and } V \to V_g \end{aligned}$$

For convenience, we can consider a new height variable $z' = z - h_s$ and express the ordinary differential equation and boundary conditions as follows:

$$\frac{d^2W_a}{dz'^2} - \frac{if}{K}W_a = 0$$

$$\begin{aligned} &\text{at } z' = 0,\ W_a = U_s - U_g - iV_g \\ &\text{as } z' \to \infty,\ W_a \to 0 \end{aligned}$$

The general solution to the above differential equation is

$$W_a = A\exp[-(1 + i)az'] + B\exp[(1 + i)az']$$

in which the constants A and B are determined from the boundary conditions as

$$A = U_s - U_g - iV_g;\ B = 0$$

Substituting these in the above solution and decomposing it into real and imaginary parts, we obtain

$$U = U_g - e^{-az'}[(U_g - U_s)\cos(az') + V_g \sin(az')]$$
$$V = V_g + e^{-az'}[(U_g - U_s)\sin(az') - V_g \cos(az')]$$

An important physical condition to be satisfied by the velocity distribution in the PBL is that the shear stress vector must be parallel to the wind vector near the surface. This requires that

$$\text{at } z' = 0, \ \tau_{zy} = 0, \ \text{or } \frac{\partial V}{\partial z'} = 0$$

This condition yields the following relationship between the geostrophic wind components and the actual near-surface wind:

$$U_g + V_g = U_s$$

combining it with the usual relationship

$$U_g^2 + V_g^2 = G^2$$

the geostrophic wind components can be determined as

$$U_g = \tfrac{1}{2}[U_s + (2G^2 - U_s^2)^{1/2}]$$
$$V_g = \tfrac{1}{2}[U_s - (2G^2 - U_s^2)^{1/2}]$$

after ignoring the other unphysical roots of the quadratic equations for U_g and V_g (note that, in the northern hemisphere, $U_g > - V_g > 0$).

Using the given parameter values, we can obtain from the above expressions

$$U_g = 9.64 \text{ m s}^{-1} \text{ and } V_g = -2.64 \text{ m s}^{-1}$$

which imply that the cross-isobar angle near the surface (at $z = h_s$, or $z' = 0$)

$$\alpha_o = \tan^{-1}(-V_g/U_g) \cong 15.4°$$

is much smaller than 45° given by the original Ekman solution. This is a consequence of the different lower boundary condition used here.

The Ekman boundary layer height is given as

$$h = \pi\left(\frac{2K}{f}\right)^{1/2} \cong 628 \text{ m}$$

Then, using the already derived expressions for U and V, it is easy to calculate and plot the profiles of U and V as functions of z from 10 m to h or even a higher level, if desired.

7.6 Developing Laminar Boundary Layers

In the simple cases of plane-parallel flows discussed in Sections 7.4 and 7.5, inertial accelerations or forces are zero and there is a balance between the pressure gradient and friction forces, or between pressure gradient, Coriolis, and friction forces. As a result, thickness of the affected fluid layer does not change in the flow direction or x–y plane. In developing viscous flows, such as boundary layers, wakes, and jets, the thickness of the layer in which viscous or friction effects are important changes in the direction of flow, and inertial forces are as important, if not more, as the viscous forces. The ratio of the two defines the Reynolds number $\text{Re} = UL/\nu$, where U and L are the characteristic velocity and length scales (there may be more than one length scale characterizing the flow). This ratio is a very important characteristic of any viscous flow and indicates the relative importance of inertial forces as compared to viscous forces.

Atmospheric boundary layers developing over most natural surfaces are characterized by very large (10^6–10^9) Reynolds numbers. Boundary layers encountered in engineering practice also have fairly large Reynolds numbers ($\text{Re} = 10^3$–10^6, based on the boundary layer thickness as the length scale and the ambient velocity just outside the boundary layer as the velocity scale). One would expect that in such large Reynolds number flows the nonlinear inertia terms in the equations of motion will be far greater in magnitude than the viscous terms, at least in a gross sense. Still, it turns out that the viscous effects cannot be ignored in order to satisfy the no-slip boundary condition and to provide a smooth transition, through the boundary layer, from zero velocity at the surface to finite ambient velocity outside the boundary layer. Recognizing this, Prandtl (1905) first proposed an important boundary layer hypothesis which states that, under rather broad conditions, viscosity effects are significant in layers adjoining solid boundaries and in certain other layers (e.g., mixing layers and jets), the thicknesses of which approach zero as the Reynolds number of the flow approaches infinity, and are small outside these layers. This hypothesis has been applied to a variety of flow fields and is supported by many observations. The thickness of a boundary or mixing layer should be looked at in relation to the distance over which it develops. This explains the existence of relatively thick boundary layers in the atmosphere, in spite of very large Reynolds numbers characterizing the same.

The boundary layer hypothesis, for the first time, explained most of the dilemmas of inviscid flow theory, and clearly defined regions of the flow where such a theory may not be applicable and other regions where it would provide close simulations of real fluid flows. It also provided a practically useful definition of the boundary layer as the layer in which the fluid velocity makes a transition from that of the boundary (zero velocity, in the case of a fixed boundary) to that appropriate for an ambient (inviscid) flow. In theory, as well as in practice, the approach to ambient velocity is often very smooth and asymptotic, so that some arbitrariness or ambiguity is always involved in defining the boundary layer thickness. In engineering practice, the outer edge of the boundary layer is usually taken where the mean velocity has attained 99% of its ambient value. This definition is found to be quite unsatisfactory in meteorological applications, where other more useful definitions of the boundary layer thickness have been used (e.g., the Ekman layer thickness defined earlier).

Prandtl's boundary layer hypothesis is found to be valid for laminar as well as turbulent boundary layers. The fact that the boundary layer is thin compared with the distance over which it develops along a boundary allows for certain approximations to be made in the equations of motion. These boundary layer approximations, also due to Prandtl, amount to the following simplifications for the viscous diffusion terms in Equation (7.4):

$$
\begin{aligned}
\nu\nabla^2 u &\cong \nu(\partial^2 u/\partial z^2) \\
\nu\nabla^2 v &\cong \nu(\partial^2 v/\partial z^2) \qquad (7.32)\\
\nu\nabla^2 w &\cong \nu(\partial^2 w/\partial z^2)
\end{aligned}
$$

which follow from the neglect of velocity gradients parallel to the boundary in comparison to those normal to it.

7.6.1 The flat-plate laminar boundary layer

Let us consider the simple case of a steady, two-dimensional boundary layer developing over a thin flat plate placed in an otherwise steady, uniform stream of fluid, with streamlines of the ambient flow parallel to the plate (see Figure 7.4). This is an important classical case of fluid flow which provides a standard

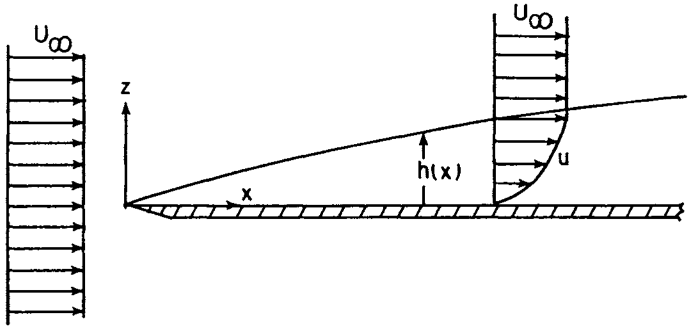

Figure 7.4 Schematic of a developing boundary layer over a flat plate.

for comparison with boundary layers developing on slender bodies, such as aircraft wings, ship hulls, and turbine blades. Except in a small region near the edge of the plate, where boundary layer approximations may not be valid, the relevant boundary layer equations to be solved are

$$\begin{aligned} u(\partial u/\partial x) + w(\partial u/\partial z) &= \nu(\partial^2 u/\partial z^2) \\ \partial u/\partial x + \partial w/\partial z &= 0 \end{aligned} \tag{7.33}$$

with the boundary conditions

$$\begin{aligned} u = w = 0, &\quad \text{at } z = 0 \\ u \to U_\infty, &\quad \text{as } z \to \infty \\ u = U_\infty, &\quad \text{at } x = 0, \quad \text{for all } z \end{aligned}$$

where U_∞ is the uniform ambient velocity just outside the boundary layer.

Some idea about the growth of the boundary layer with distance downstream of the leading edge can be obtained by requiring that the inertial and viscous terms of Equation (7.32) be of the same order of magnitude in the boundary layer, i.e.,

$$u(\partial u/\partial x) \sim \nu(\partial^2 u/\partial z^2)$$

or

$$U_\infty^2/x \sim \nu U_\infty/h^2$$

or

$$h \sim (\nu x/U_\infty)^{1/2} = x/\mathrm{Re}_x^{1/2} \tag{7.34}$$

where $\mathrm{Re}_x = U_\infty x/\nu$ is a local Reynolds number. The above result indicates that the boundary thickness grows in proportion to the square root of the distance and that the ratio h/x decreases inversely proportional to the square root of the local Reynolds number. This supports the idea of a thin boundary layer in a large Reynolds number flow.

Equation (7.32) can be solved numerically. The resulting velocity profiles at various distances from the edge of the plate turn out to be similar in the sense that they collapse onto a single curve if the normalized longitudinal velocity u/U_∞ is plotted as function of the normalized distance z/h, or $z/(\nu x/U_\infty)^{1/2}$, from the surface. If, to begin with, one assumes a similarity solution of the form

$$u/U_\infty = f'(\eta) = \partial f/\partial \eta \tag{7.35}$$

where $\eta = z(U_\infty/\nu x)^{1/2}$, it is easy to show that the partial differential equations [Equation (7.33)] yield a single ordinary differential equation

$$f''' + \tfrac{1}{2} f f'' = 0 \tag{7.36}$$

where prime denotes differentiation with respect to η. The boundary conditions can be transformed to

$$\begin{aligned} f = f' &= 0, \quad \text{at } \eta = 0 \\ f' &\to 1, \quad \text{as } \eta \to \infty \end{aligned}$$

The normalized velocity profile obtained from the numerical solution of the above equations is shown in Figure 7.5. Note that the profile near the plate surface is nearly linear, similar to the velocity profiles in Ekman layers and plane-parallel flows (this linearity of profiles seems to be a common feature of all laminar flows). The shear stress on the plate surface is given by

$$\tau_0 = \mu(\partial u/\partial z)_{z=0} = 0.33\rho U_\infty^2 \, \mathrm{Re}_x^{-1/2} \tag{7.37}$$

according to which the friction or drag coefficient, $C_\mathrm{D} \equiv \tau_0/\rho U_\infty^2$, varies inversely proportional to the square root of the local Reynolds number. The boundary layer thickness (defined as the value of z where $u = 0.99U_\infty$) is given by

$$h \cong 5(\nu x/U_\infty)^{1/2} \tag{7.38}$$

Many measurements in flat-plate laminar boundary layers have confirmed these theoretical results (Schlichting, 1960).

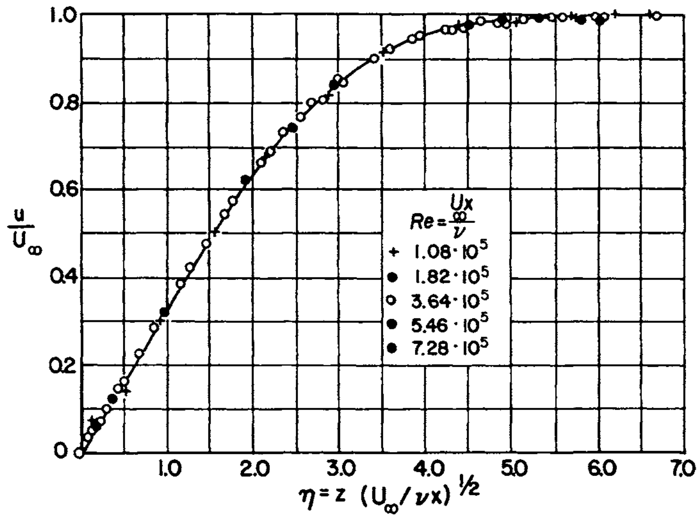

Figure 7.5 Comparison of theoretical and observed velocity profiles in the laminar flat-plate boundary layer. [From Schlichting (1960).]

7.7 Heat Transfer in Laminar Flows

In Section 4.4 we derived the one-dimensional equation of heat conduction in a solid medium and pointed out how it can be generalized to three dimensions. Heat transfer in a still fluid is no different from that in a solid medium, molecular conduction or diffusion being the only mechanism of transfer. In a moving fluid, however, heat is more efficiently transferred by fluid motions while thermal conduction is a relatively slow process.

7.7.1 Forced convection

Consideration of conservation of energy in an elementary fluid volume, in a Cartesian coordinate system, leads to the following equation of heat transfer in a low-speed, incompressible flow in which temperature or heat is considered only a passive admixture not affecting in any way the dynamics.

$$DT/Dt = \alpha_h \nabla^2 T \tag{7.39}$$

where α_h is the molecular thermal diffusivity of the fluid and the total derivative has the usual meaning as defined by Equation (7.5) and incorporates the important contribution of fluid motions.

Equation (7.39) describes the variation of temperature for a given velocity field and can be solved for the appropriate boundary conditions and flow situations. Analytical solutions are possible only for certain types of laminar flows. For two-dimensional thermal boundary layers, jets, and plumes the boundary layer approximations are used to simplify Equation (7.39) to the form

$$u(\partial T/\partial x) + w(\partial T/\partial z) = \alpha_h(\partial^2 T/\partial z^2) \tag{7.40}$$

which is similar to the simplified boundary layer equation of motion.

Analogous to the Reynolds number, one can define the Peclet number $\mathrm{Pe} = UL/\alpha_h$, which represents the ratio of the advection terms to the molecular diffusion terms in the energy equation. Instead of Pe, it is often more convenient to use the Prandtl number $\mathrm{Pr} = \nu/\alpha_h$, which is a property of the fluid only and not of the flow; note that

$$\mathrm{Pe} = \mathrm{Re} \times \mathrm{Pr} \tag{7.41}$$

For air and other diatomic gases, $\mathrm{Pr} \cong 0.7$ and is nearly independent of temperature, so that the Peclet number is of the same order of magnitude as the Reynolds number.

The difference in the temperature at a point in the flow and at the boundary is usually normalized by the temperature difference ΔT across the entire thermal layer and is represented as a function of normalized coordinates of the point, the appropriate Reynolds number, and the Prandtl number. The heat flux on a boundary is usually represented by the dimensionless ratio, called the Nusselt number

$$\mathrm{Nu} = H_0 L/k\Delta T \tag{7.42}$$

or, the heat transfer coefficient

$$C_H = H_0/\rho c_p U \Delta T \tag{7.43}$$

which is also called the Stanton number. Note that the above parameters are related (through their definitions) as

$$C_H = \mathrm{Nu}/\mathrm{RePr} = \mathrm{Nu}/\mathrm{Pe} \tag{7.44}$$

Many calculations, as well as observations of heat transfer in pipes, channels, and boundary layers have been used to establish empirical correlations between the Nusselt number or the heat transfer coefficient as a function of the Reynolds and Prandtl numbers. Some of these have found practical applications in micrometeorological problems, particularly those dealing with heat and mass transfer to or from individual leaves (Lowry, 1970; Monteith, 1973; Gates, 1980; Monteith and Unsworth, 1990).

7.7.2 *Free convection*

In free or natural convection flows, temperature cannot be considered as a passive admixture, because inhomogeneities of the temperature field in the presence of gravity give rise to significant buoyant accelerations that affect the dynamics of the flow, particularly in the vertical direction. This is usually the case in the atmosphere. The equations of motion and thermodynamic energy are slightly modified to allow for the buoyancy effects of temperature or density stratification. It is generally assumed that there is a reference state of the atmosphere at rest characterized by temperature T_0, density ρ_0, and pressure p_0, which satisfy the hydrostatic equation

$$\partial p_0/\partial z = -\rho_0 g \tag{7.45}$$

and that, in the actual atmosphere, the deviations in these properties from their reference values ($T_1 = T - T_0$, $\rho_1 = \rho - \rho_0$ and $p_1 = p - p_0$) are small compared to the values for the reference atmosphere ($T_1 \ll T_0$, $\rho_1 \ll \rho_0$, etc). These Boussinesq assumptions lead to the approximation

$$(1/\rho)(\partial p/\partial z) + g \cong (1/\rho_0)(\partial p_1 \partial z) + (g/\rho_0)\rho_1 \tag{7.46}$$

which can be used in the vertical equation of motion. In an ideal gas, such as air, changes in density are simply related to changes in temperature as

$$\rho_1 = -\beta\rho_0 T_1 \cong -(\rho_0/T_0)T_1 \tag{7.47}$$

in which the coefficient of thermal expansion $\beta = -(1/\rho_0)(\partial\rho/\partial T)p \cong 1/T_0$. After substituting from Equations (7.46) and (7.47) in the equation of vertical motion [Equation (7.4)], we have

$$Dw/Dt = -(1/\rho_0)(\partial p_1/\partial z) + (g/T_0)T_1 + \nu\nabla^2 w \tag{7.48}$$

Here, the second term on the right-hand side is the buoyant acceleration due to the deviation of temperature from the reference state. The equations of horizontal motion remain unchanged; alternatively, one can replace the pressure gradient terms $(1/\rho)(\partial p/\partial x)$ and $(1/\rho)(\partial p/\partial y)$ by $(1/\rho_0)(\partial p_1/\partial x)$ and

$(1/\rho_0)(\partial p_1/\partial y)$, respectively. A more appropriate form of the thermodynamic energy equation, for micrometeorological applications, is

$$D\theta/Dt = \alpha_h \nabla^2 \theta \tag{7.49}$$

in which θ is the potential temperature.

The above equations are valid for both stable and unstable stratifications. In the particular case of true free convection over a flat plate (horizontal or vertical) in which the motions are entirely generated by surface heating, the relevant dimensionless parameters on which temperature and velocity fields depend are the Prandtl number and the Grashof number

$$\mathrm{Gr} = (g/T_0)(L^3 \Delta T/\nu^2) \tag{7.50}$$

Instead of Gr, one may also use the Rayleigh number

$$\mathrm{Ra} = (g/T_0)(L^3 \Delta T/\nu\alpha_h) = \mathrm{Gr} \times \mathrm{Pr} \tag{7.51}$$

Both the Grashof and Rayleigh numbers are expected to be large in the atmosphere, although true free convection in the sense of no geostrophic wind forcing may be a rare occurrence.

7.8 Applications

Since micrometeorology deals primarily with the phenomena and processes occurring within the atmospheric boundary layer, some familiarity with the fundamentals of viscous and inviscid flows is essential. In particular, the basic differences between viscous and inviscid flows and between laminar and turbulent viscous flows should be recognized. The Navier–Stokes equations of motion and the thermodynamic energy equation and difficulties of their solution must be familiar to the students of micrometeorology. Introduction to some of the fundamentals of fluid flow and heat transfer may provide a useful link between dynamic meteorology and fluid mechanics. A direct application of this might be in micrometeorological studies of momentum, heat, and mass transfer between the atmosphere and the physical and biological elements (e.g., snow, ice, and water surfaces and plant leaves, animals, and organisms).

Problems and Exercises

1. In what regions or situations in the atmosphere may the inviscid flow theory not be applicable and why?

2. What are the basic difficulties in the solution of the Navier–Stokes equations of motion for laminar viscous flows?

3. Distinguish between the following types of environmental fluid flows, giving an example of each type from the atmosphere:
(a) inviscid and viscous flows;
(b) laminar and turbulent flows;
(c) forced and free convection.

4. In the gravity flow down an inclined plane, determine the volume flow rate Q across the plane per unit width of the plane and express the layer depth h as a function of Q and the slope angle β.

5.
(a) What are the various limitations of the classical Ekman-layer solution when compared to observations in the atmospheric boundary layer.
(b) Discuss different ways of improving the theoretical solution to the equation of motion for the PBL.

6. Using the solution to the equations of mean horizontal motion in the PBL given in the worked-out Example Problem 2, calculate and plot the following:
(a) The cross-isobar angle near the surface as a function of the ratio U_s/G.
(b) Profiles of normalized velocity components U/G and V/G as functions of height z up to 1000 m for the parametric values given in the example problem, which are typical of a neutral PBL.
(c) Velocity component profiles for a stable boundary layer of height $h = 100$ m and $U_s/G = 0.35$, using the appropriate value of K for the given h. Compare these with those for the neutral case in (b).

7.
(a) By direct substitution verify that Equation (7.29) is a solution to Equation (7.27) which satisfies the boundary conditions [Equations (7.28)].
(b) Using the above solution [Equation (7.29)], obtain the corresponding expressions for the horizontal shear stress components τ_{zx} and τ_{zy}.
(c) Show that in a coordinate system with the x axis parallel to the surface shear stress (this implies that $\tau_{zx} = \tau_0$ and $\tau_{zy} = 0$, at $z = 0$), $U_g = G/\sqrt{2}$, $V_g = -G/\sqrt{2}$, and $\tau_0 = \rho G(\nu f)^{1/2}$.
(d) In the same coordinate system write down the expressions for the normalized velocity components (u/G and v/G) and the normalized shear stress components (τ_{zx}/τ_0 and τ_{zy}/τ_0).
(e) Using the above expressions, calculate and plot the vertical profiles of the normalized velocity and shear stress components as functions of az from 0 to 2π.

(f) What conclusions can you draw from the above profiles? Comment on their applicability to the real atmosphere, if ν can be replaced by an effective viscosity K.

8. Starting from the equations of motion with boundary-layer approximations, derive Equation (7.36) for the dimensionless velocity profile in a flat-plate boundary layer.

9.

(a) What Boussinesq assumptions or approximations are commonly used to simplify the equations of motion in a thermally stratified environment.

(b) Derive the approximate expression (7.46) and discuss its usefulness and application to modeling small-scale atmospheric flows.